Adaptive Antiviral Immunity Is a Determinant of the Therapeutic Success of Oncolytic Virotherapy

Paul T Sobol[1], Jeanette E Boudreau[2], Kyle Stephenson[2], Yonghong Wan[2], Brian D Lichty[2] and Karen L Mossman[1,2]

[1]Department of Biochemistry and Biomedical Sciences, McMaster University, Hamilton, Ontario, Canada; [2]Department of Pathology and Molecular Medicine, Centre for Gene Therapeutics, McMaster University, Hamilton, Ontario, Canada

Oncolytic virotherapy, the selective killing of tumor cells by oncolytic viruses (OVs), has emerged as a promising avenue of anticancer research. We have previously shown that KM100, a Herpes simplex virus type-1 (HSV) deficient for infected cell protein 0 (ICP0), possesses substantial oncolytic properties *in vitro* and has antitumor efficacy *in vivo,* in part by inducing antitumor immunity. Here, we illustrate through T-cell immunodepletion studies in nontolerized tumor-associated antigen models of breast cancer that KM100 treatment promotes antiviral and antitumor $CD8^+$ cytotoxic T-cell responses necessary for complete tumor regression. In tolerized tumor-associated antigen models of breast cancer, antiviral $CD8^+$ cytotoxic T-cell responses against infected tumor cells correlated with the induction of significant tumoristasis in the absence of tumor-associated antigen-specific $CD8^+$ cytotoxic T-cells. To enhance oncolysis, we tested a more cytopathic ICP0-null HSV and a vesicular stomatitis virus M protein mutant and found that despite improved *in vitro* replication, oncolysis *in vivo* did not improve. These studies illustrate that the *in vitro* cytolytic properties of OVs are poor prognostic indicators of *in vivo* antitumor activity, and underscore the importance of adaptive antiviral $CD8^+$ cytotoxic T-cells in effective cancer virotherapy.

Received 16 June 2010; accepted 31 October 2010; published online 30 November 2010. doi:10.1038/mt.2010.264

INTRODUCTION

Oncolytic virotherapy, which involves the selective killing of cancerous cells by viruses, is a promising avenue of anticancer research. Although Herpes simplex virus type-1 (HSV)-based oncolytic viruses (OVs) have been shown to be safe with promising efficacies in clinical trials, research is required to understand how OVs successfully mediate tumor regression.

Recent studies have underscored the importance of the infected cell protein 0 (ICP0) in counteracting type I interferon (IFN)-mediated blocks to viral replication.[1,2] IFNs upregulate a variety of IFN-stimulated genes that in turn mediate its antiviral and antiproliferative effects.[3–5] IFN unresponsiveness is also often a consequence of carcinogenesis, allowing the tumor to subvert these proapoptotic and antiproliferative effects.[6–9] These observations provided a basis for developing OVs lacking proteins key for inhibiting the host IFN response, such as M protein mutants of vesicular stomatitis virus (VSVΔM51) and ICP0-null HSV.[7,10]

During OV infection *in vivo*, tumor-associated antigens (TAAs) liberated by oncolysis are internalized by antigen-presenting cells and proteolytically processed into immunodominant peptides that are presented on the cell surface by MHC I. Upon migration to local lymph nodes, antigen-presenting cells present these peptides to $CD8^+$ T-cells, driving their proliferation and expansion into effector, or cytotoxic T-lymphocytes (CTLs), and memory populations. CTLs home to the tumor where they bind to MHC I:peptide complexes on tumor cell membranes. Upon successful recognition of these complexes, CTLs release granules containing perforin and granzyme to induce cytolysis, allowing OVs to indirectly drive antitumor immunity.[11–14]

Many replication-defective virus-based cancer immunotherapeutics have been developed to express peptides derived from CTL epitopes of TAAs.[15] Although sustained CTL responses are initiated, the frequency and persistence of these responses are low and do not necessarily correlate with improved clinical outcome.[15,16] These poor therapeutic results are largely due to mechanisms of peripheral and central tolerance that dampen TAA-specific CTL responses, as well as the poor binding affinity and immunogenicity of TAA immunodominant epitopes.[17–20] By re-engineering OVs to express endogenous TAAs, or foreign antigens expressed in the tumor or only by the OV, it was hoped that these tolerogenic mechanisms could be overcome and tumor regression could be achieved.[21–24] However, few of these studies have assessed the therapeutic contribution of CTL responses against OV-derived immunogenic proteins in the stringent context of tolerized TAA models of cancer. Since viral proteins are foreign, immunologic tolerance wouldn't apply, allowing for increased binding and improved tumor regression. Recent research illustrated that vaccination strategies utilizing OVs encoding immunogenic model antigens like ovalbumin are effective therapeutically,[23] and that the genomes and antigens from OVs persist long after treatment,[25–29] further underscoring the potential utility of OV-derived immunogenic proteins as adopted tumor cell targets.

Correspondence: *Karen L Mossman, Department of Pathology and Molecular Medicine, MDCL 5026, 1200 Main St.W., Hamilton, Ontario, Canada L8N 3Z5. E-mail: mossk@mcmaster.ca*

We have shown that ICP0-null HSV possesses oncolytic properties in cancer cells harboring defects in the type I IFN response *in vitro* and *in vivo* in the polyoma middle T antigen murine model of breast cancer.[10,30] Upon characterization of the requirements for ICP0-null HSV oncolysis *in vivo* in nontolerized and tolerized TAA models of breast cancer, we found that antitumor and antiviral CTL responses in nontolerized TAA models led to tumor regression whereas antiviral CTL responses in tolerized TAA models led to tumoristasis. Furthermore, the sensitivities of cancer cell lines to *in vitro* oncolysis by ICP0-null HSV and VSVΔM51 mutants were poor predictors of *in vivo* antitumor activities. This study underscores the importance of selecting tumor models that faithfully recapitulate tumor immunological phenomena for *in vivo* studies of antitumor properties of viruses.

RESULTS

In vitro oncolytic activities of ICP0-null HSV in two breast cancer cell models

The molecular basis for tumor-selective killing by OVs is dependent on tumor-associated defects in antiviral cytokine signaling pathways, including IFN.[31] We have previously shown that the ICP0-null HSV KM100 possesses *in vivo* antitumor properties in the polyoma middle T antigen breast cancer model,[32] with complete tumor regression occurring in 80% of mice and concomitantly with a humoral immune response.[10] Although these and other studies underscored the importance of defective IFN signaling in tumor cell permissiveness to KM100 oncolysis, the exact nature of the antitumor immune response remained unknown.[10,30]

Toward evaluating the *in vivo* antitumor properties of KM100 in other murine breast cancer models, we first assayed the *in vitro* cytopathic effects of KM100 in HER-2/*neu* breast tumor explants and in the *neu*$^{OT\text{-}I/OT\text{-}II}$ breast carcinoma cell line NOP32. Primary HER-2/*neu* and NOP32 cells were infected with KM100, wild-type (wt) HSV (KOS) for a positive control of cell death, or an ICP0-null HSV (n212) to compare the cytolytic properties of a less-attenuated HSV. Although all cell types were sensitive to KOS infection at all multiplicities of infection (MOIs), both tumor cell cultures were relatively insensitive to KM100 infection, with an MOI of 10 required to induce 50% cytopathic effects (**Figure 1a**). n212 infection resulted in an intermediate level of tumor cell death, as cytolysis occurred at MOIs as low as 0.5. These results were recapitulated when viral titers were quantified (**Figure 1b**) and correlated with the IFN responsiveness of both tumor types (**Figure 1c**). As KM100 is an IFN-sensitive OV, it is not surprising that both cell cultures were relatively resistant to oncolysis at low MOIs. Though measurable differences in the IFN responsiveness of HER-2/*neu* tumor and NOP32 cultures was evident, they may be due to the presence of contaminating fibroblasts in the HER-2/*neu* primary tumor explant cultures.

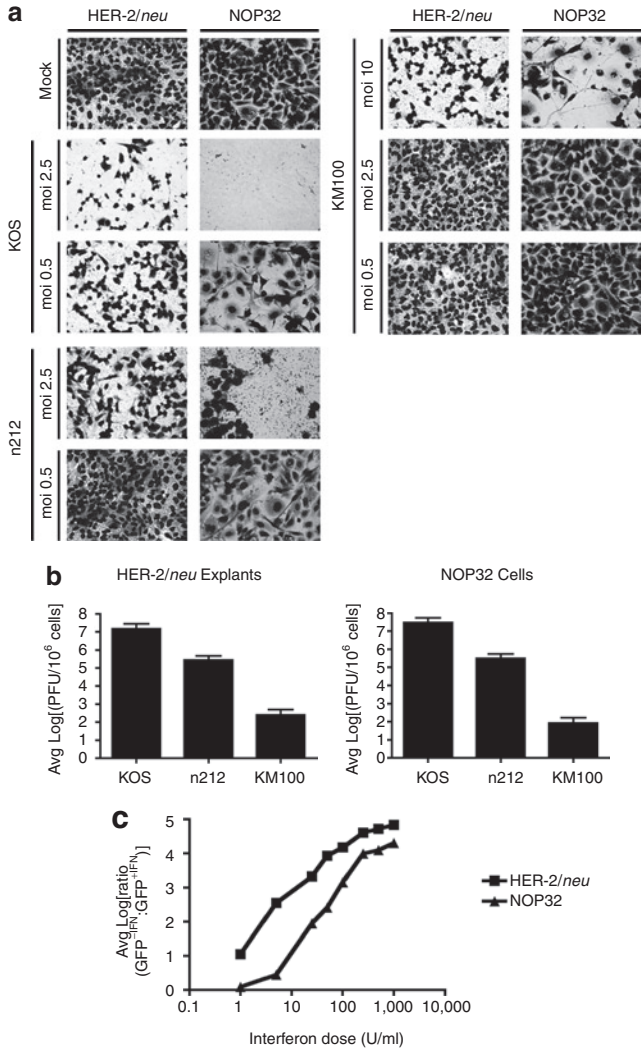

Figure 1 KM100 displays limited oncolytic activity in IFN-responsive NOP32 cells and HER-2/*neu* primary tumor explants cells. (**a**) HER-2/*neu* tumor explant cells and the *neu*$^{OT\text{-}I/OT\text{-}II}$ transgenic cell line NOP32 were infected at varying multiplicities of infection (MOIs) for 3 days with wild-type Herpes simplex virus strain KOS, the infected cell protein 0-null HSV n212, or the oncolytic KM100, and cytopathic effects were visualized by Giemsa staining. (**b**) Parallel cultures of HER-2/*neu* and NOP32 cells were infected at a MOI of 2.5 and harvested for quantification of total infectious virus by plaque assay. Data are expressed as means ± SD. Limit of detection of plaque assay, $\log_{10} = 2.3$ (**c**) Interferon (IFN) responsiveness assays were performed as in Materials and Methods. Shown are the average, log-transformed green fluorescent protein (GFP) fluorescence ratios of tumor cell cultures pretreated with regular growth medium (–IFN) or with varying doses of IFN (+IFN) from three experiments performed in triplicate. Low ratio values denote cellular IFN unresponsiveness. Data are representative of three independent experiments.

In vivo antitumor activity of KM100 in nontolerized TAA models of breast cancer

Having ascertained the *in vitro* oncolytic activities of ICP0-null HSVs, we next evaluated their antitumor properties *in vivo*. HER-2/*neu* tumor-bearing wt FVB mice were intratumorally treated with either KM100 or n212 and tumor growth was measured until complete regression was achieved or until established endpoint parameters were observed. Treatment of HER-2/*neu* tumors with either KM100 or n212 significantly increased survival of tumor-bearing mice compared to mock treated tumor-bearing mice (**Figure 2a**). However, no significant differences in survival were noted between the two treatment groups, irrespective of the ICP0-null HSV virus used (KM100 or n212) or of the dose of virus administered (2×10^6 pfu or 2×10^7 pfu) (**Figure 2a** and data not shown). Tumor growth was stabilized until 20 days post-ICP0-null HSV treatment for all groups (**Figure 2b**), with complete

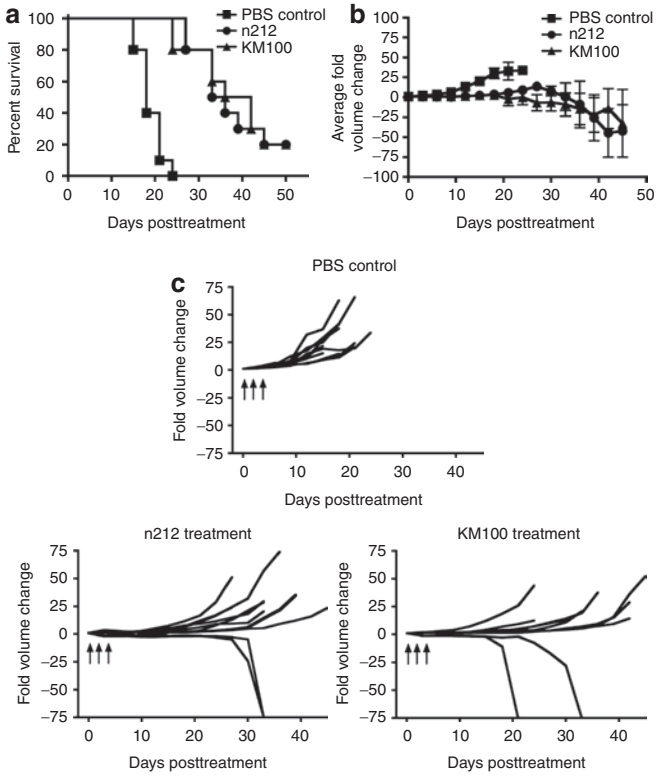

Figure 2 Infected cell protein 0–null herpes simplex viruses (HSVs) possess equivalent *in vivo* antitumor properties in the HER-2/*neu* murine breast cancer model. Subcutaneous HER-2/*neu* breast tumor-bearing wt FVB mice were intratumorally treated with three doses of 2×10^7 pfu of either n212 or KM100 or an equivalent amount of phosphate-buffered saline (PBS) on days 0, 1 and 3. (**a**) Kaplan–Meier survival analysis of ICP0-null HSV treatments. Statistical significance was determined by the log-rank test, where $P < 0.05$. (**b**) Intergroup comparisons of the fold changes in HER-2/*neu* tumor volume within each ICP0-null HSV or PBS control group. Statistical significance was determined by the Koziol distribution free test when $P < 0.001$.[33] (**c**) Intragroup comparisons of the fold changes in HER-2/*neu* tumor volume measurements between the PBS control (upper panel), n212 (lower left), and KM100 (lower right) treatment groups. Error bars indicate SE of experimental means within treatment groups from **a** and **b**. Arrows indicate time of virus injection. Data were generated from 10 mice per treatment group, combined from two independent experiments.

regression occurring in 20% of mice in each treatment group (Figure 2c). Intergroup comparison of tumor growth illustrated statistically significant differences between all virus treatment groups and the phosphate-buffered saline (PBS) control treated mice, as determined by the Koziol distribution free statistical test (Figure 2b).[33] All mice that completely regressed their tumors were subsequently challenged with a subcutaneous injection of 10^6 HER-2/*neu* tumor cells at 80 days postviral treatment, and found to be refractory to this tumor rechallenge. Taken together, these data demonstrate that ICP0-null HSVs possess antitumor activities in the nontolerized HER-2/*neu* murine breast cancer model.

KM100-induced antitumor immunity depends on the induction of TAA-specific CTLs in a nontolerized TAA model of breast cancer

We next investigated the contribution of individual T-cell subsets to KM100-induced antitumor immunity. $CD8^+$, $CD4^+$, or $CD8^+$ and $CD4^+$ T-cells were immunodepleted *in vivo* in HER-2/*neu* tumor-bearing wt FVB mice and challenged with intratumoral administration of KM100. We did not observe any significant differences in the rates of HER-2/*neu* tumor growth of the immunodepleted mice relative to PBS control or total rat IgG isotype control administered mice (Figure 3 and data not shown). To ensure that both T-cell subsets were sufficiently depleted, splenic lymphocytes were isolated and analyzed for cell surface expression of CD3 and either CD4 or CD8 by flow cytometry. $CD8^+$ T-cell depletion, but not $CD4^+$ T-cell depletion, significantly abrogated the antitumor properties of KM100 (Figure 3a). These results were confirmed by intergroup comparisons of tumor growth across the treatment groups, with significant differences occurring between the $CD8^+$ T-cell depleted groups and control and $CD4^+$ T-cell depleted groups (Figure 3b), and intragroup comparisons of tumor growth after KM100 treatment, with complete regression occurring in 20% to 30% of non-$CD8^+$ T-cell depleted groups (Figure 3c). These data demonstrate the importance of $CD8^+$ T-cells in establishing antitumor immunity after KM100 administration.

KM100 induces OV- and tumor-specific CTLs in a nontolerized TAA model of breast cancer

Since $CD8^+$ T-cell depletion completely ablated the *in vivo* antitumor properties of KM100, we next evaluated the roles for CTLs in antitumor and anti-HSV immunity. Splenocytes from HER-2/*neu* tumor-bearing wt FVB mice were recovered 8 days post-KM100 treatment and the percentages of HER-2/*neu*-specific and HSV-specific $CD8^+$ T-cells were enumerated by intracellular IFN-γ staining following restimulation with either the $CD8^+$ T-cell immunodominant peptide derived from HER-2/*neu* (PDSLRDLSVF) or purified HSV lysate. *Ex vivo* restimulation with both HER-2/*neu* immunodominant peptide and HSV lysate was capable of driving antigen-specific intracellular IFN-γ expression in CTLs, whereas unstimulated cells or those treated with an irrelevant peptide derived from lymphocytic choriomeningitis virus (LCMV) gp-1 (KAVYNFATC) did not (Figure 3d and data not shown). These data not only indicate KM100 primes CTL responses to HER-2/*neu*, but that this is crucial to establishing therapeutic antitumor immunity.

KM100 possesses limited *in vivo* antitumor activity and fails to induce TAA-specific CTLs in a tolerized TAA model of breast cancer

In agreement with other studies, we have shown OVs are capable of mounting TAA-specific immune responses mediated by CTLs in nontolerized TAA cancer models (Figure 3).[21] Given that CTLs eliminate virally infected cells by mediating TAA- or viral antigen-dependent killing following peptide:MHC I recognition, it is not surprising that $CD8^+$ T-cell immunodepletion severely abrogated tumor regression following KM100 administration. Since a major barrier to successful antitumor immunity following therapeutic TAA vaccination involves central and peripheral tolerance, we investigated whether KM100 possesses antitumor properties in cancer models that faithfully recapitulate TAA and tissue-specific immunological tolerance. Therefore, we treated HER-2/*neu* tumor-bearing transgenic FVB HER-2/*neu*-202 (FVB-N202) mice with

KM100 and monitored tumor growth and animal survival. KM100 treatment not only significantly improved the survival of FVB-N202 mice (**Figure 4a**; $P < 0.05$), but also significantly reduced HER-2/*neu* tumor growth (**Figure 4b**; $P < 0.001$). However, complete tumor regression was not observed in KM100-treated FVB-N202 mice (**Figure 4c**).

Given the roles for $CD8^+$ T-cells in the regression of HER-2/*neu* tumors in nontolerized wt mice (**Figure 3a,b,c**), we investigated the induction of TAA-specific CTLs in the tolerized TAA tumor model. As determined by intracellular IFN-γ staining, while a large proportion of splenic CTLs were specific for HSV antigen, few were specific for the neu CTL epitope (**Figure 4d**). Previous research found that vaccination with the HER-2/*neu* immunodominant peptide induced protective, high-avidity antitumor CTLs in nontolerized wt FVB mice but not in tolerized transgenic FVB-N202 mice.[34] Similarly, the capacity of KM100 to liberate TAAs and/or elicit antitumor CTL responses was impaired in transgenic FVB-N202 mice.

To recapitulate this effect in another mouse strain, and to expand this work to another OV, we studied the oncolytic properties of KM100 and VSVΔM51 in the tolerized TAA breast cancer model $neu^{OT\text{-}I/OT\text{-}II}$ in C57/BL6 mice.[35] Spontaneous $neu^{OT\text{-}I/OT\text{-}II}$ mammary tumors and cell lines derived thereof express the rat neu oncoprotein fused at its C-terminus to the $CD8^+$ (OT-I) and $CD4^+$ (OT-II) T-cell epitopes from the model antigen ovalbumin. Ovalbumin-specific T-cell responses are then used as surrogate markers for antitumor T-cell responses.[35] The NOP32 cell line was derived from a $neu^{OT\text{-}I/OT\text{-}II}$ primary tumor whose *in vivo* growth was arrested after OT-I and OT-II T-cell adoptive transfer, and therefore displays a stable disease phenotype.[35] Although both KM100 and VSVΔM51 are capable of infecting NOP32 cells, this cell line is relatively insensitive to oncolysis *in vitro* at low MOIs (**Figure 1** and **Supplementary Figure S1**).

We treated NOP32 tumor-bearing transgenic $neu^{OT\text{-}I/OT\text{-}II}$ mice with VSVΔM51 or KM100 and monitored tumor growth and animal survival. Both VSVΔM51 and KM100 treatment significantly improved the survival of $neu^{OT\text{-}I/OT\text{-}II}$ mice ($P < 0.05$; **Figure 5a**) and reduced NOP32 tumor growth ($P < 0.001$; **Figure 5b**). Like the tolerized FVB-N202 model (**Figure 4**), treatment of $neu^{OT\text{-}I/OT\text{-}II}$ mice with either OV failed to induce both complete tumor regression (**Figure 5c**) and antitumor CTL responses, as measured by intracellular IFN-γ staining of CTLs restimulated with the ovalbumin $CD8^+$ T-cell immunodominant peptide, SIINFEKL (**Figure 5d**). Similar to KM100 treatment of HER-2/*neu* tumors in transgenic FVB-N202 mice, VSVΔM51 and KM100 treatment of NOP32 tumors in $neu^{OT\text{-}I/OT\text{-}II}$ mice elicited potent antiviral CTL responses, as determined by intracellular IFN-γ staining of HSV glycoprotein B–specific (HSV gB) and VSV nucleoprotein (NP)-specific CTLs in the peripheral blood. In an effort to translate these studies into a nontolerized model, we attempted to engraft wt C57BL/6 mice with NOP32 tumors and found that engraftment rates were very

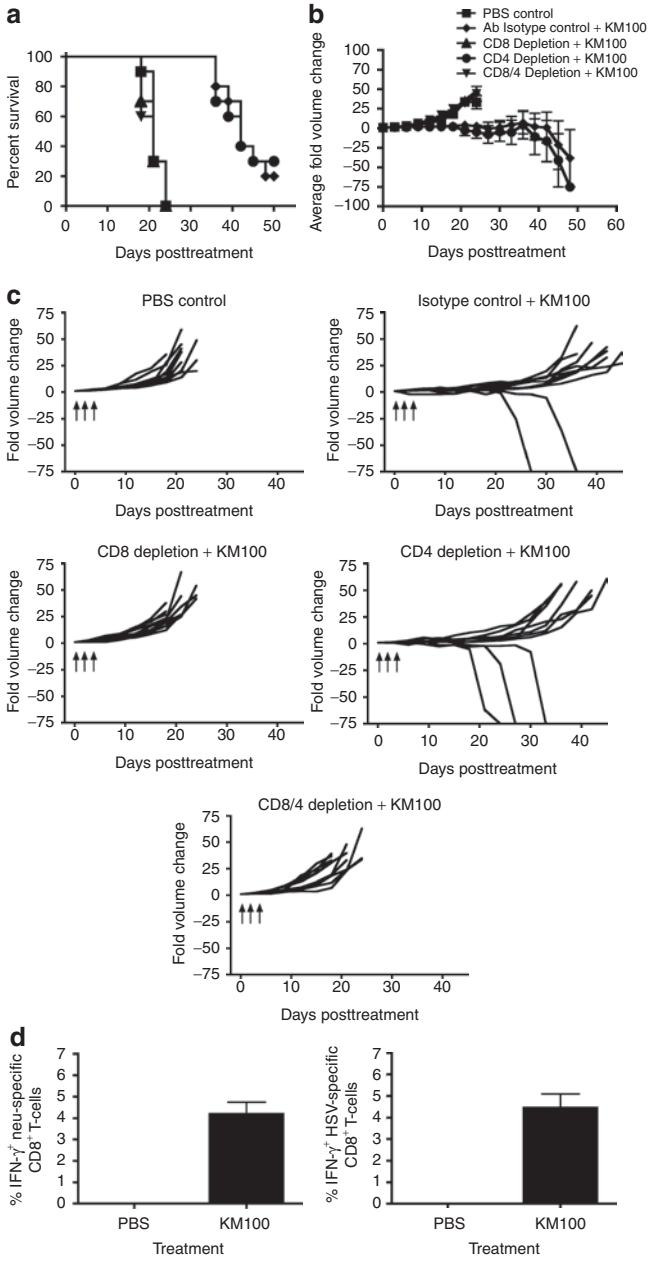

Figure 3 The *in vivo* antitumor properties of KM100 are dependent on $CD8^+$ T-cells in the HER-2/*neu* breast cancer model. Individual components of the T-cell compartment were immunodepleted in HER-2/*neu* tumor-bearing wild-type mice as in Materials and Methods, and three doses of 2×10^7 pfu of KM100 were administered intratumorally as in **Figure 2**. (**a**) Kaplan–Meier survival analysis of T-cell-depleted animals, isotype control antibody (rat IgG) and phosphate-buffered saline (PBS) administered mice following KM100 treatment. Statistical significance was determined by the log-rank test, where $P < 0.05$. (**b**) Intergroup comparisons of the average fold changes in HER-2/*neu* tumor volume within each KM100 or PBS control group. Statistical significance was determined by the Koziol distribution free test when $P < 0.001$.[33] (**c**) Intragroup comparisons of the fold changes in HER-2/*neu* tumor volume measurements between the control and KM100 treatment groups. Error bars indicate SE of experimental means within treatment groups from **a** and **b**. Arrows indicate time of injection. Antibody-only administration had no significant effects on fold changes in tumor volume or survival. (**d**) Splenocytes from HER-2/*neu* tumor-bearing wt mice treated 8 days earlier with KM100 were restimulated *ex vivo* with the H2-D^q-restricted $CD8^+$ T-cell immunodominant epitope peptides of neu (left panel), Herpes simplex virus (HSV) lysate (right panel) or an irrelevant peptide (LCMV gp-1; data not shown), and HER-2/neu- and HSV-specific $CD8^+$ T-cells were enumerated by intracellular IFN-γ staining. Error bars represent the SE of experimental means. Data were generated from 10 mice per treatment group, combined from two independent experiments.

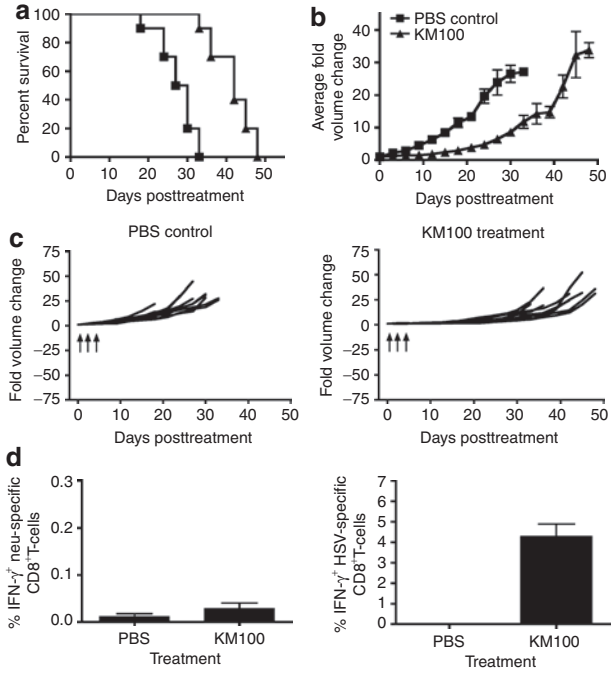

Figure 4 KM100 possesses limited *in vivo* antitumor properties in the tolerized HER-2/*neu* tumor antigen breast cancer model. Subcutaneous HER-2/*neu* tumor-bearing transgenic FVB-N202 mice were intratumorally treated with 2×10^7 pfu of KM100 as in **Figure 2**. (**a**) Kaplan–Meier survival analysis of KM100 treatments. Statistical significance was determined by the log-rank test, where $P < 0.05$. (**b**) Intergroup comparisons of the fold changes in HER-2/*neu* tumor volume within each treatment group. Statistical significance was determined by the Koziol distribution free test when $P < 0.001$.[33] (**c**) Intragroup comparisons of the fold changes in HER-2/*neu* tumor volume measurements between the phosphate-buffered saline (PBS) control (left panel) and KM100 (right panel) treatment groups. Error bars indicate SE of experimental means within treatment groups from **a** and **b**. Arrows indicate time of injection. (**d**) Splenocytes from HER-2/*neu* tumor-bearing HER-2/*neu* transgenic FVB mice treated 8 days earlier with KM100 were restimulated *ex vivo* with the H2-D^q-restricted CD8$^+$ T-cell immunodominant epitope peptide of neu (left panel), HSV lysate (right panel) or an irrelevant peptide (lymphocytic choriomeningitis virus gp-1; data not shown), and HER-2/neu- and HSV-specific CD8$^+$ T-cells were enumerated by intracellular interferon-γ (IFN-γ) staining. Error bars represent the SE of experimental means. Data were generated from two experiments involving 5 mice per treatment group.

low. Of the engrafted tumors, 60% regressed following treatment with PBS (data not shown), thereby indicating that the presence of the highly immunogenic neu$^{OT\text{-}I/OT\text{-}II}$ chimeric protein biased the immune response. These data indicate VSVΔM51 and KM100 possess *in vivo* tumoristatic properties in tolerized TAA models of breast cancer that coincide with the induction of antiviral, but not antitumor, CTL responses.

Antiviral CTLs may potentiate tumoristasis in tolerized TAA cancer models and commence rejection in nontolerized TAA cancer models

Although neither VSVΔM51 nor KM100 were capable of inducing the levels of tumor-specific CTLs required to drive complete tumor regression in either tolerized TAA breast cancer model, the prominent induction of antiviral CTLs in all models tested may have allowed for tumoristasis. To determine whether the

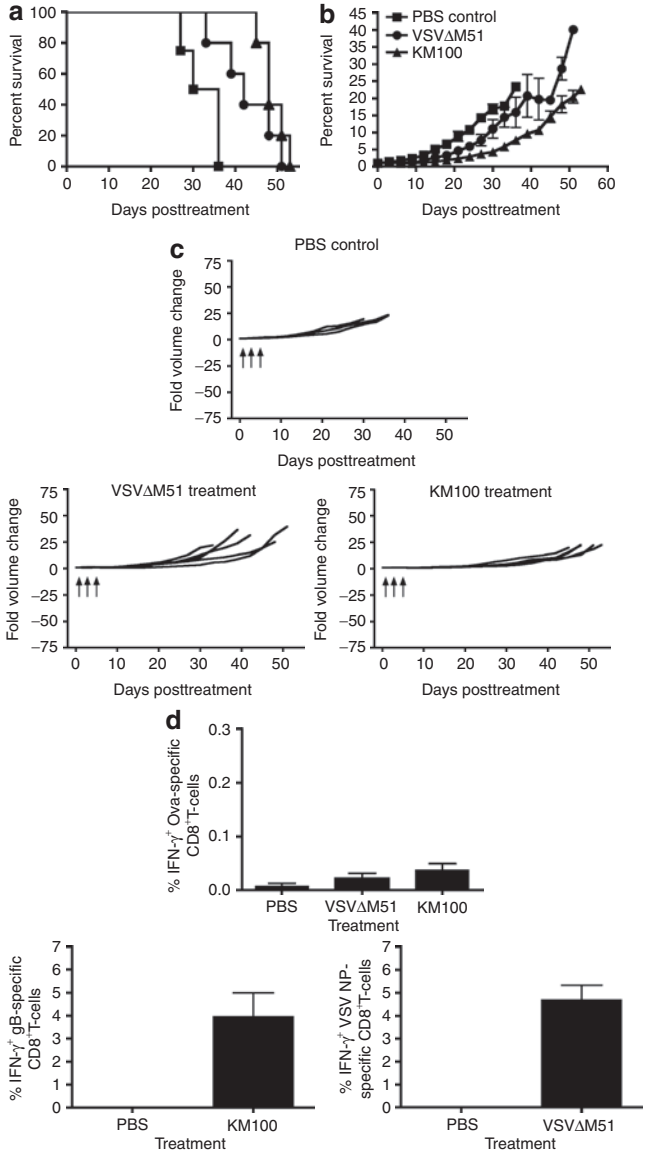

Figure 5 KM100 possesses limited *in vivo* antitumor properties in the neuOT-I/OT-II transgenic breast cancer model. Subcutaneous NOP32 tumor-bearing *neu*$^{OT\text{-}I/OT\text{-}II}$ transgenic mice were intratumorally treated with 2×10^7 pfu of KM100 or 5×10^8 pfu VSVΔM51 as in **Figure 2**. (**a**) Kaplan–Meier survival analysis of oncolytic virus treatments. Statistical significance was determined by the log-rank test, where $P < 0.05$. (**b**) Intergroup comparisons of the fold changes in NOP32 tumor volume within each treatment group. Statistical significance was determined by the Koziol distribution free test when $P < 0.001$.[33] (**c**) Intragroup comparisons of the fold changes in NOP32 tumor volume measurements between the phosphate-buffered saline (PBS) control (upper panel), VSVΔM51 (lower left) and KM100 (lower right) treatment groups. Error bars indicate SE of experimental means within treatment groups from **a** and **b**. Arrows indicate time of injection. Data were generated from five mice per treatment group, and four mice from the PBS control group. (**d**) Peripheral blood mononuclear cells from NOP32 tumor-bearing *neu*$^{OT\text{-}I/OT\text{-}II}$ transgenic FVB mice treated 8 days earlier with either VSVΔM51 or KM100 were restimulated *ex vivo* with the H2-K^b–restricted CD8$^+$ T-cell immunodominant epitope peptides of ovalbumin (OVA) (upper panel), vesicular stomatitis virus (VSV) nucleoprotein (lower right), herpes simplex virus glycoprotein B (HSV gB) (lower left) or an irrelevant peptide (lymphocytic choriomeningitis virus gp-1; data not shown), and OVA-, VSV- and HSV-specific CD8$^+$ T-cells were enumerated by intracellular interferon-γ (IFN-γ) staining. Error bars represent the SE experimental means. Data were generated as in **a** and **c**.

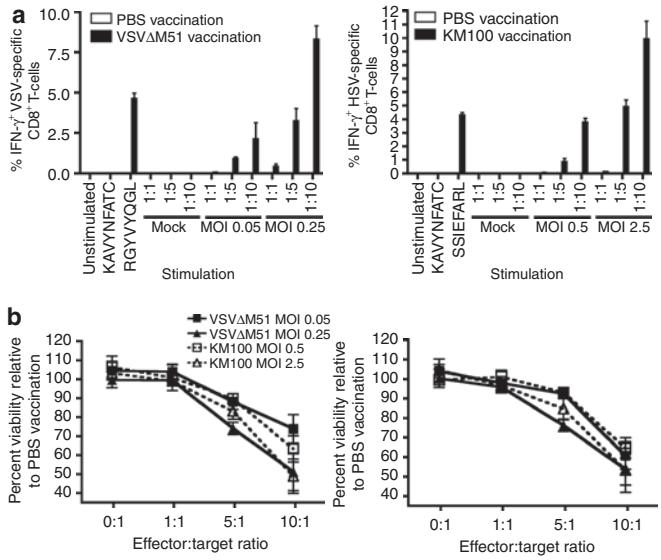

Figure 6 Oncolytic virus-mediated protein presentation to CD8$^+$ T-cells is sufficient for tumor cell death. Female wt C57BL/6 mice were subcutaneously vaccinated with three injections of either 5 × 10^8 pfu VSVΔM51 or 2 × 10^7 pfu KM100. Ten days later, the local superficial inguinal lymph nodes and spleens were harvested, and MAC-sorted CD8α$^+$ pooled splenocytes were cocultured in the presence of NOP32 cells infected with the corresponding oncolytic virus. (**a**) IFN-γ staining of CD8$^+$ T-cells cocultured with VSVΔM51-infected (left panel) or KM100-infected NOP32 cells (right panel) at the indicated multiplicities of infection (MOIs). (**b**) Cellular viability of VSVΔM51- or KM100-infected NOP32 cells cocultured with CD8$^+$ T-cells from **a** as determined by 5-carboxyfluorescein diacetate-acetoxymethyl ester staining for membrane integrity (left panel) and alamar Blue staining for cellular metabolism (right panel). Errors bars denote SE of experimental means. Data are representative of two experiments. PBS, phosphate-buffered saline; VSV, vesicular stomatitis virus, IFN, interferon.

presentation of immunodominant KM100 and VSVΔM51 proteins were capable of driving the selective killing of OV-infected tumor cells, we performed *ex vivo* HSV gB epitope or VSV NP epitope presentation assays. C57BL/6 mice were subcutaneously vaccinated with three doses of VSVΔM51 or KM100, and after 10 days their splenocytes and inguinal lymph nodes were recovered. MAC-sorted CD8α$^+$ T-cells were cocultured with NOP32 cells infected with VSVΔM51 or KM100 at MOIs that are insufficient for oncolysis (**Figure 1**, and **Supplementary Figure S1**). After 2 days, HSV gB or VSV NP epitope presentation to CD8$^+$ T-cells was gauged by intracellular IFN-γ staining and CTL tumor killing was measured by two cellular viability assays: 5-carboxyfluorescein diacetate-acetoxymethyl ester (CFDA-AM) staining, which measures cellular membrane integrity, and alamar Blue staining, which measures cellular metabolism. Vaccination of C57BL/6 mice with either KM100 or VSVΔM51 induced large proportions of HSV- and VSV-reactive CTLs that recognized KM100- or VSVΔM51-infected NOP32 cells, respectively (**Figure 6a**). This OV antigen presentation occurred concomitantly with significant reductions in the metabolic rate and membrane integrity of the NOP32 tumor cells relative to cocultures containing T-cells derived from PBS-vaccinated mice (**Figure 6b**). We also compared the capacity for both bulk splenocytes and CD8α$^+$ T-cells from mice vaccinated with KM100 to kill VSVΔM51-infected NOP32 cells and found that at no effector:target ratio did cells isolated from KM100-vaccinated mice kill VSVΔM51-infected NOP32 cells and vice versa (data not shown). These data indicate that OV infection of NOP32 cells did not elicit a general effect on the sensitivity of these cells to killing by T-cells. In addition, splenocytes negatively sorted for CD8α from OV-vaccinated mice were found to be entirely incapable of killing NOP32 tumor cells infected with the respective OV at effector-to-target ratios as high as 10:1. These studies also illustrated expression of immunogenic OV proteins is sufficient for breast tumor cell lysis in the presence of OV-specific CTL, and underscore the potential utility of OV-specific CTL in mediating tumor growth suppression in the absence of tumor-specific CTLs. In an effort to determine whether OV antigens persisted in NOP32 tumors following either KM100 or VSVΔM51 treatment, immunohistochemical staining of pan-HSV and VSV antigens was employed. As illustrated in **Supplementary Figure S2**, pockets of tumor cells positively immunostained for HSV antigens for up to 45 days after the last dose of KM100 was intratumorally administered and 33 days post-VSVΔM51 treatment. Taken together with other studies that documented long-lasting OV antigen persistence occurring concomitantly with OV-induced tumoristasis,[25–29] it is likely that antiviral CTLs mediate durable, lasting tumoristasis in the presence of immunological and tolerogenic barriers that limit epitope spreading to TAAs.

DISCUSSION

Given the lack of success of existing cancer immunotherapeutics, it is worthwhile to examine the immune mechanisms that mediate the complex interplay between OVs, the tumor microenvironment and their hosts. Previous studies illustrated the importance of the immune system in mediating indirect tumor regression by various OVs, but few have investigated the specific contributions of antiviral and antitumor immunities in tolerized TAA models.

We found that KM100 possessed substantial antitumor properties in the nontolerized HER-2/*neu* model, with 20% of mice completely regressing their tumors. To improve this therapeutic effect, we compared the antitumor properties of KM100 and n212, an ICP0-null HSV mutant that retains VP16 function and replicates more efficiently than KM100, particularly under low multiplicity conditions (**Figure 1**).[36] Only n212 was capable of mediating cytolysis at MOIs achievable *in vivo* in HER-2/*neu* tumor cells *in vitro*. However, KM100 was at least as capable as n212 at curing mice, improving their lifespan and inducing tumor regression *in vivo*, despite the large replicative advantage of n212. Although this finding would indicate that the *in vivo* antitumor properties of OVs are dependent on criteria beyond cytolysis-driven TAA liberation, additional studies need to be undertaken to assess the antitumor properties of n212 and KM100 administered at lower doses, as it is possible that the viral doses used may have been too high to discriminate between the viruses.

Although not as immunogenic as the polyoma middle T antigen, we reasoned that the rat HER-2/*neu* oncoprotein could potentially drive a misleading CTL response against the tumor. KM100 treatment not only induced a potent adaptive antiviral CTL response, but also substantial antitumor CTL responses that were sufficient for tumor regression and subsequent tumor protection. Although this observation is in agreement with other studies

showing that multiple OVs are capable of inducing an impressive TAA-specific immune response mediated by CTLs against primary[11–14,21–23,37] and metastatic tumors,[38] our immunodepletion studies illustrated no contribution for $CD4^+$ T-cells in KM100-induced antitumor immunity. Although in apparent disagreement with other studies,[13] our results may be specific to the particular models of breast cancer used to study oncolysis, the OV vector used and the depletion or knockout methodological approaches used. Although antiviral $CD4^+$ T-cells would very likely play a role in priming and maintaining CTL activities, CTLs would nevertheless be the direct effector immune cell population involved in tumoristasis.

To transpose these results into the corresponding tolerized TAA breast cancer model, we treated HER-2/*neu* tumor-bearing transgenic FVB-N202 mice. Although we could not detect antitumor CTL responses, KM100 treatment induced potent antiviral responses and significantly abrogated tumor growth and improved survival. These results were recapitulated in the tolerized TAA breast cancer model $neu^{OT\text{-}I/OT\text{-}II}$ in C57BL/6 mice. Furthermore, VSVΔM51, another promising OV, induced substantial tumoristatic effects independent of an antitumor CTL response. Therefore, these findings are independent of the mouse strain, tolerized TAA cancer model or OV used. These studies indicate the *in vivo* antitumor properties of OVs are more dependent on the tumor immunological context than their intrinsic cytolytic capacities *in vitro*. Our data imply that CTL responses generated as a result of OV administration are better predictors of *in vivo* efficacy than are the kinetics of *in vitro* OV replication.

The failure of these OVs to induce TAA-specific CTL responses in tolerized antigen cancer models are most likely due to central tolerance to the neu oncogene, or forms of peripheral tolerance such as local immunosuppression mediated by transforming growth factor-β and interleukin-10.[39,40] $CD4^+CD25^+$ T-regulatory cells, in particular, substantially dampen HER-2/*neu*-specific CTL recruitment to the tumor following HER-2/*neu* vaccination in HER-2/*neu* tumor-bearing transgenic N202 mice.[34] T-cells that are reactive to TAAs may also become exhausted and dysfunctional due to chronic stimulation within the tumor microenvironment.[41,42] Despite the existence of these immunological barriers to complete regression and the absence of antitumor CTL responses, we observed significant tumoristasis following OV treatment. We hypothesize that tumor cells expressing foreign viral antigens stimulate $CD8^+$ T-cells that are not susceptible to the same central tolerance mechanisms that delete autoreactive T-cells, or to exhaustion following chronic stimulation from the tumor. Tumor cells would express this novel antigen upon OV administration, making them targets for the immune system as virally infected cells. The cumulative effects of lytic reactivation by HSV-based OVs and persistent viral antigen presentation by OV-infected tumor cells would then allow for a protracted antiviral response, abrogating tumor growth.[25–29]

The induction of OV-specific CTLs *in vivo* was sufficient to kill infected tumor cells *in vitro* at relatively low effector:target ratios. These data indicate that the expression and MHC I–restricted presentation of immunodominant OV proteins likely mediate tumoristasis in tolerized TAA cancer models *in vivo*. However, the presence of immunological barriers to tumor rejection, such as $CD4^+CD25^+$ T-regulatory cells, may limit the necessary epitope spreading of CTL responses to TAAs required for complete tumor regression. This could potentially be overcome by coadministration of OVs with chemotherapeutic agents that favour epitope spreading, such as anthracyclins.[43]

In summary, these data indicate the *in vitro* cytolytic capacity of OVs and antiviral cytokine sensitivities of tumor cells are poor prognostic indicators of the *in vivo* antitumor properties of viruses on those tumor cell populations. Instead, central and peripheral forms of immunological tolerance to TAAs are the key determinants of whether an OV can induce antitumor CTL responses. These studies underscore the importance of selecting appropriate cancer models that faithfully recapitulate tumor immunological phenomena to study the *in vivo* antitumor properties of OVs and that failure to do so biases the immunological response to OV treatment due to the lack of natural systemic and local immunosuppression. Although these immunological barriers prevent complete tumor regression by OVs, the induction of OV-specific CTL responses likely provide for tumor growth stabilization and tumoristasis. These data not only highlight the significance of antiviral CTL responses against OV-infected tumor cells *in vivo*, but also illustrate the potential importance of epitope spreading from OV antigens to immunodominant TAAs. Rather than developing OVs with improved replicative capacities *in vitro*, it would be more beneficial to develop multi-modal anticancer platforms that promote epitope spreading from immunodominant OV antigens to TAAs.

MATERIALS AND METHODS

Peptides. Peptides used include the $CD8^+$ T-cell immunodominant epitope $OVA_{257–264}$ peptide [SIINFEKL (2 μg/ml); Pepscan Systems; Lelystad, the Netherlands], the H2-D^q-restricted $CD8^+$ T-cell immunodominant epitope $neu_{420–429}$ peptide [PDSLRDLSVF (2 μg/ml); Pepscan Systems],[44] the H2-K^b–restricted $CD8^+$ T-cell immunodominant epitope of HSV $gB_{498–505}$ peptide [SSIEFARL (8 μg/ml); Pepscan Systems],[45] the H2-K^b–restricted $CD8^+$ T-cell epitope vesicular stomatitis virus nucleoprotein $NP_{498–505}$ peptide [RGYVYQGL; Biomer Technologies; Hayward, CA], or an irrelevant peptide derived from the H2-K^b–restricted $CD8^+$ T-cell immunodominant epitope of LCMV gp-$1_{33–41}$ (KAVYNFATC; Biomer Technologies).[46]

Cell culture. Human osteosarcoma cells (U2OS; American Type Culture Collection; ATCC, Manassas, VA) and African Green Monkey kidney epithelial cells (Vero; ATCC) were maintained in Dulbecco's modified Eagle's media (DMEM) supplemented with 10% fetal bovine serum (FBS). NOP32 cells were grown in DMEM containing 10% FBS and 1:50 *w*/*v* B-27 supplement (Gibco, Carlsbad, CA), while HER-2/*neu* tumor explant cells were grown in DMEM supplemented with 10 ng/ml epidermal growth factor (Gibco). All media contained 2 mmol/l L-glutamine, 100 U/ml penicillin, and 100 μg/ml streptomycin (all Gibco). All cell lines were grown at 37 °C under humidified conditions.

Virus culture. HSV recombinants used in these studies include wt strain KOS (KOS), KM100 ($ICP0^{n212}VP16^{in1814}$)[36] and the ICP0-null mutant n212, which was generated by *icp0* allele deletions through linker insertion.[47] KOS was propagated in Vero cells, while KM100 and n212 were propagated on U2OS cells in the presence of 3 mmol/l hexamethylene bisacetamide (Sigma; St. Louis, MO). All HSV-1 constructs were purified and concentrated via sucrose cushion ultracentrifugation. VSV recombinants used for experimentation include VSV strain Indiana expressing GFP under the VSV genome promoter (VSVgfp) and the corresponding M protein mutant (VSVΔM51gfp). Both VSV constructs were propagated on Vero

cells, and purified and concentrated via sucrose cushion ultracentrifugation. For HSV and VSV viral infections, cells were seeded into either 12- or 24-well dishes 24 hours prior to infection at 37 °C under humid conditions. Cells were then infected in serum-free DMEM for 1 hour at the indicated MOI, at which point fresh 5% FBS DMEM growth medium was replaced.

Murine tumor models. All animal work was performed in full compliance with the Canadian Council on Animal Care and approved by the Animal Research Ethics Board of McMaster University. HER-2/*neu* tumor cells were surgically isolated from HER-2/*neu* transgenic mice that spontaneously develop mammary adenocarcinomas (FVB-N202; Jackson Laboratories, Bar Harbor, MN)[48]. Tumor explants were grown to confluence in DMEM supplemented with 10% FBS and 10 ng/ml epidermal growth factor (Gibco). Monolayers were trypsinized and rinsed twice in ice-cold PBS. A total of 11 HER-2/*neu* tumor explant cultures were created at various times for experimentation, with the same culture isolates being used within each dataset described in a figure. All tumor explant cultures were equivalently sensitive to KM100 infection. For *in vivo* modeling, cell suspensions were concentrated to 1×10^6 cells/200 µl and injected into the left flank of either 6–8 week old female wt FVB mice or transgenic FVB-N202 mice (Jackson Laboratories). Once tumors reached an approximate ellipsoid volume of 65 mm^3, mice were injected intratumorally with 50 µl PBS or virus as indicated. Tumor volumes were determined by the following formula, which is representative of an ellipsoid:(4/3) (π) (length) ((width)^2). Regression analyses were plotted as tumor growth curves over time and represent average fold increases or decreases in tumor volume. *neu*$^{OT\text{-}I/OT\text{-}II}$ C57BL/6 mice[35] were received from B. Nelson and bred at the McMaster Central Animal Facility according to Canadian Council on Animal Care regulations. The genotypes of these mice were confirmed throughout the breeding process by PCR analysis for the presence or absence of the neu oncogene using primers specific for the neu gene. Six- to eight-week-old heterozygous *neu*$^{OT\text{-}I/OT\text{-}II}$ mice were injected with 10^6 NOP32 cells into the left flank. Treatment conditions and tumor volume measurements were completed as previously described for the HER-2/*neu* tumor model.

Interferon responsiveness assays. Sub-confluent cell cultures were incubated in the presence of varying amounts of human IFN-α (Sigma) for 12 hours and subsequently challenged with infection by the IFN-sensitive virus VSV expressing gfp (VSVgfp). Twenty-four hours later, GFP fluorescence was quantified in cell cultures as a direct measure of the capacity for cell types to respond to IFN treatment using a Typhoon Trio Variable Mode Imager (Amersham Biosciences, Piscataway, NJ). Mean GFP fluorescence intensities were normalized to those of mock treated (noninfected) samples. The relative ratio of GFP fluorescence in cultures untreated to those pretreated with IFN was subsequently calculated. Briefly, if a cell type is unresponsive to IFN pretreatment, then the replicative capacity of VSV and the intensity of GFP fluorescence would be approximately equivalent to those cultures pretreated with media alone.

Cytopathic effect and plaque assays. Cytopathic effects were measured 3 days postinfection following methanol fixation and Giemsa staining (Sigma) unless otherwise indicated. Viral titers from parallel cultures were measured via plaque assays. Total virus (cell and supernatant) was harvested by three rounds of freeze-thawing, followed by centrifugation at 3,000 rpm for 5 minutes. ICP0-null HSV samples were serially diluted on U2OS cells in the presence of 3 mmol/l hexamethylene bisacetamide, and cell monolayers were maintained in DMEM supplemented with 2% human serum (Gibco), 3 mmol/l hexamethylene bisacetamide and 1% FBS. KOS was titered on Vero cells in the absence of hexamethylene bisacetamide. After the indicated times postinfection, cells were methanol-fixed and Giemsa-stained to allow for plaque quantification.

Cellular viability assays. The fluorescent indicator dyes alamar Blue (Medicorp, Montreal, CA) and CFDA-AM (Molecular Probes, Eugene, OR) were used to evaluate the cellular metabolic rate and intracellular esterase activity of treated cultures, respectively.[49] At the indicated times posttreatment, culture supernatants were aspirated and replaced with 4 µmol/l CFDA-AM and 5% w/v alamar Blue diluted in PBS. The cells were scanned with a Safire fluorometric plate reader (Tecan, Raleigh, NC) after a 1 hour incubation, where the excitation and emission wavelengths for alamar Blue were 530 nm and 595 nm, respectively, while those of CFDA-AM were 485 nm and 530 nm, respectively.

T-cell depletion assays. Depletions of different components of the T-cell compartment in HER-2/*neu* tumor-bearing mice were completed using purified monoclonal antibodies derived from hybridomas obtained from the ATCC: GK1.5 (anti-CD4) and 2.43 (anti-CD8α). One hundred (GK1.5) or two hundred (2.43) micrograms were injected intraperitoneally either 7 days (2.43) or 2 days (GK1.5) before viral challenge and then twice a week for the duration of the experiment. Total rat IgG (Sigma) was used as a control antibody treatment. In an effort to assess the efficiencies of the depletions, the indicated lymphocyte classes in peripheral blood mononuclear cells were investigated by flow cytometric analysis of cell surface staining for CD3 and CD4 or CD3 and CD8.

Immunohistochemistry. Mice were sacrificed at varying times post-OV treatment, and NOP32 tumors were resected and frozen in Tissue-Tek Optimal Cutting Temperature media (Ted Pella, Redding, CA) in liquid nitrogen. Cryosections were cut at 10 µm thickness using a cryostat and were fixed in 3% paraformaldehyde for 15 minutes at room temperature, washed in Tris-buffered saline (TBS), and incubated at room temperature in 3% hydrogen peroxide diluted in methanol. After two 5-minute washes in TBS, sections were blocked in 5% goat serum TBS for 1 hour at room temperature, and then incubated with polyclonal rabbit primary antibodies diluted in blocking buffer overnight at 4 °C. Primary antibodies used were specific for HSV antigens (1:2,500, DAKO, Carpinteria, CA) or VSV antigens (1:2,500 of polyclonal serum),[50] as indicated. After hybridization, sections were washed three times with TBS, and immunostaining was detected using the DAKO Envision detection kit (DAKO). Immunostained sections were washed three times with TBS, and sections were developed using AEC chromogen, immersed in distilled water and counterstained with hematoxylin according to the manufacturer's instructions. Images of positively immunostained tumor sections were captured using a Leica DM IRE2 microscope.

Cell surface and intracellular cytokine staining. Peripheral blood was harvested from mice 8 days following T-cell immunodepletion by submandibular or retro-orbital bleeding. To each blood sample, 2 ml of ACK lysis buffer (150 mmol/l NH_4Cl, 10 mmol/l $KHCO_3$, 100 mmol/l Na_2EDTA, pH 7.3) was added. After 5 minutes, Hanks Balanced Salt Solution was added and cultures were spun at 1,500 rpm for 10 minutes. Pellets were resuspended in ACK lysis buffer, and incubated for an additional 5 minutes, diluted in Hanks Balanced Salt Solution and centrifuged again at 1,500 rpm for 10 minutes. Cells were then surface stained with CD4-PE-Cy5 Ab (1:200; clone RM4-5), rat anti-mouse CD8-PE-Cy7 Ab (1:100; clone 53-6.7) and CD3-APC-Cy7 Ab (1:100; clone 145-2C11; all BD Biosciences, Mississauga, CA) in FACS buffer (0.5% bovine serum albumin in PBS) for 30 minutes on ice. Cells were then washed with FACS buffer, fixed and permeabilized with Cytofix/Cytoperm (BD Biosciences) for 20 minutes on ice. After two washes with Cytoperm solution, cells were resuspended in FACS buffer and filtered. Data were acquired using a FACS LSRII flow cytometer and FACSDiva flow data acquisition software and analyzed using FlowJo software (Tree Star, Ashland, OR). Splenocytes from individual treated mice were harvested, dissociated and incubated in ACK buffer, diluted in Hanks Balanced Salt Solution and centrifuged at 1,500 rpm for 10 minutes. Cell pellets were resuspended in 10% FBS RPMI, plated at a density of 2×10^6 cells per well and restimulated with 1 µg/ml of the aforementioned peptides or 20 µg/ml of HSV lysate for 5 hours at 37 °C. Cultures were incubated in the presence of GolgiPlug and

anti-CD28 antibody (all BD Biosciences). Cells were then treated with FcBlock, cell surface stained as above, washed with FACS buffer and fixed and permeabilized with Cytofix/Cytoperm (BD Biosciences) for 20 minutes on ice. Cells were then washed twice with Cytoperm solution (BD Biosciences) and incubated with IFN-γ-APC Ab (1:100 in Permwash buffer; clone XMG1.2, BD Biosciences) for 30 minutes on ice. After two washes with Cytoperm solution, cells were resuspended in FACS buffer and filtered. Data were acquired using a FACS LSRII flow cytometer and FACSDiva flow data acquisition software and analyzed using FlowJo software.

Viral antigen presentation assay. Naive C57BL/6 mice were subcutaneously vaccinated three times with either 2×10^7 pfu of KM100, 5×10^8 pfu VSVΔM51 or PBS in 50 µl, with injections made 36 hours apart. Ten days after the first injection, spleens and inguinal lymph nodes were removed, and pooled cultures were positively selected for CD8α by magnetic-activated cell sorting using a Vario magnetic-activated cell sorter (Miltenyi Biotec, Bergisch Gladbach, GR) and a CD8α$^+$ T-cell magnetic-activated cell sorting isolation kit (Miltenyi Biotec) according to the manufacturer's recommendations. Confirmation of homogeneity and cell surface phenotype was performed using flow cytometric analysis of CD3, CD4, and CD8 expression as described above. NOP32 tumor cells were infected with either VSVΔM51 or KM100 at the indicated MOIs for 16 hours as described above, washed three times in PBS, and then cocultured with CD8α$^+$ splenocytes in 10% FBS RPMI. Cocultured cells were plated at target-to-effector cell ratios of 1:1, 1:5, and 1:10 in a 96-well plate, where 5×10^4 target cells were plated per well. For control purposes, CD8α$^+$ splenocytes were plated in the presence of 100 ng/well of phorbol myristate acetate (Sigma) and 250 ng/well of ionomycin (Sigma) in a 50 µl volume with effector cells to ensure cytokine production. A positive control for viral antigen-specific cytokine release involved incubation of effector and target cells with 1 µg/ml of either the immunodominant peptides of HSV gB (SSIEFARL), VSV nucleoprotein (RGYVYQGL) or LCMV gp-1 (KAVYNFATC). Cultures were treated with Brefeldin A and anti-CD28 antibody after 1 hour, and incubated for 12 hours. Immunoreactivity to viral antigen was tested by intracellular IFN-γ immunostaining as described above. The cellular membrane integrity and intracellular metabolic activities of target cells were determined by CFDA-AM and alamar Blue assays cellular viability assays, respectively.

Statistical analyses. All phenotypic analyses of T-cell responses, including immunodepletion experiment data, and single parametric viral replication analysis were analyzed by Student's two-tailed *t*-tests using GraphPad Prism version 4.0 (GraphPad Software, San Diego, CA). Differences between datasets involving multi-parametric analyses of viral replication were determined by either one- or two-way analyses of variance with Tukey's or Bonferroni *post hoc* tests, respectively. All animal survival datasets were evaluated by Kaplan–Meier survival analyses using log-rank tests, whereas comparisons of the changes in tumor volume between treatment groups were evaluated using Koziol distribution-free tests.[33]

SUPPLEMENTARY MATERIAL

Figure S1. Sensitivity of NOP32 cells to VSVΔM51 infection.
Figure S2. Immunohistochemical staining of OV antigens in NOP32 tumors.

ACKNOWLEDGMENTS

We would like to thank Brad Nelson for *neu*$^{OT\text{-}I/OT\text{-}II}$ mice and Derek Cummings for technical assistance. These studies were funded by the Canadian Breast Cancer Foundation, the Ontario Institute for Cancer Research and the Canadian Cancer Society. P.T.S. holds an Ontario Graduate Scholarship and J.E.B. holds a studentship from the Natural Sciences and Engineering Research Council. The authors acknowledge there are no financial conflicts of interest related to this research.

REFERENCES

1. Melroe, GT, DeLuca, NA and Knipe, DM (2004). Herpes simplex virus 1 has multiple mechanisms for blocking virus-induced interferon production. *J Virol* **78**: 8411–8420.
2. Mossman, KL, Saffran, HA and Smiley, JR (2000). Herpes simplex virus ICP0 mutants are hypersensitive to interferon. *J Virol* **74**: 2052–2056.
3. Stark, GR, Kerr, IM, Williams, BR, Silverman, RH and Schreiber, RD (1998). How cells respond to interferons. *Annu Rev Biochem* **67**: 227–264.
4. Taniguchi, T, Ogasawara, K, Takaoka, A and Tanaka, N (2001). IRF family of transcription factors as regulators of host defense. *Annu Rev Immunol* **19**: 623–655.
5. Tagliaferri, P, Caraglia, M, Budillon, A, Marra, M, Vitale, G, Viscomi, C *et al.* (2005). New pharmacokinetic and pharmacodynamic tools for interferon-α (IFN-α) treatment of human cancer. *Cancer Immunol Immunother* **54**: 1–10.
6. Stojdl, DF, Lichty, B, Knowles, S, Marius, R, Atkins, H, Sonenberg, N *et al.* (2000). Exploiting tumor-specific defects in the interferon pathway with a previously unknown oncolytic virus. *Nat Med* **6**: 821–825.
7. Stojdl, DF, Lichty, BD, tenOever, BR, Paterson, JM, Power, AT, Knowles, S *et al.* (2003). VSV strains with defects in their ability to shutdown innate immunity are potent systemic anti-cancer agents. *Cancer Cell* **4**: 263–275.
8. Dunn, GP, Sheehan, KC, Old, LJ and Schreiber, RD (2005). IFN unresponsiveness in LNCaP cells due to the lack of JAK1 gene expression. *Cancer Res* **65**: 3447–3453.
9. Li, Y, Srivastava, KK and Platanias, LC (2004). Mechanisms of type I interferon signaling in normal and malignant cells. *Arch Immunol Ther Exp (Warsz)* **52**: 156–163.
10. Hummel, JL, Safroneeva, E and Mossman, KL (2005). The role of ICP0-Null HSV-1 and interferon signaling defects in the effective treatment of breast adenocarcinoma. *Mol Ther* **12**: 1101–1110.
11. Toda, M, Rabkin, SD, Kojima, H and Martuza, RL (1999). Herpes simplex virus as an in situ cancer vaccine for the induction of specific anti-tumor immunity. *Hum Gene Ther* **10**: 385–393.
12. Nakamori, M, Fu, X, Rousseau, R, Chen, SY and Zhang, X (2004). Destruction of nonimmunogenic mammary tumor cells by a fusogenic oncolytic herpes simplex virus induces potent antitumor immunity. *Mol Ther* **9**: 658–665.
13. Miller, CG and Fraser, NW (2003). Requirement of an integrated immune response for successful neuroattenuated HSV-1 therapy in an intracranial metastatic melanoma model. *Mol Ther* **7**: 741–747.
14. Li, H, Dutuor, A, Tao, L, Fu, X and Zhang, X (2007). Virotherapy with a type 2 herpes simplex virus-derived oncolytic virus induces potent antitumor immunity against neuroblastoma. *Clin Cancer Res* **13**: 316–322.
15. Rosenberg, SA, Yang, JC and Restifo, NP (2004). Cancer immunotherapy: moving beyond current vaccines. *Nat Med* **10**: 909–915.
16. Parmiani, G, Castelli, C, Dalerba, P, Mortarini, R, Rivoltini, L, Marincola, FM *et al.* (2002). Cancer immunotherapy with peptide-based vaccines: what have we achieved? Where are we going? *J Natl Cancer Inst* **94**: 805–818.
17. Mills, KH (2004). Regulatory T cells: friend or foe in immunity to infection? *Nat Rev Immunol* **4**: 841–855.
18. Kusmartsev, S and Gabrilovich, DI (2002). Immature myeloid cells and cancer-associated immune suppression. *Cancer Immunol Immunother* **51**: 293–298.
19. Frey, AB and Monu, N (2006). Effector-phase tolerance: another mechanism of how cancer escapes antitumor immune response. *J Leukoc Biol* **79**: 652–662.
20. Mathis, D and Benoist, C (2004). Back to central tolerance. *Immunity* **20**: 509–516.
21. Diaz, RM, Galivo, F, Kottke, T, Wongthida, P, Qiao, J, Thompson, J *et al.* (2007). Oncolytic immunovirotherapy for melanoma using vesicular stomatitis virus. *Cancer Res* **67**: 2840–2848.
22. Vigil, A, Martinez, O, Chua, MA and García-Sastre, A (2008). Recombinant Newcastle disease virus as a vaccine vector for cancer therapy. *Mol Ther* **16**: 1883–1890.
23. Zhang, YQ, Tsai, YC, Monie, A, Wu, TC and Hung, CF (2010). Enhancing the therapeutic effect against ovarian cancer through a combination of viral oncolysis and antigen-specific immunotherapy. *Mol Ther* **18**: 692–699.
24. Bridle, BW, Boudreau, JE, Lichty, BD, Brunellière, J, Stephenson, K, Koshy, S *et al.* (2009). Vesicular stomatitis virus as a novel cancer vaccine vector to prime antitumor immunity amenable to rapid boosting with adenovirus. *Mol Ther* **17**: 1814–1821.
25. Varghese, S, Rabkin, SD, Nielsen, GP, MacGarvey, U, Liu, R and Martuza, RL (2007). Systemic therapy of spontaneous prostate cancer in transgenic mice with oncolytic herpes simplex viruses. *Cancer Res* **67**: 9371–9379.
26. Currier, MA, Gillespie, RA, Sawtell, NM, Mahller, YY, Stroup, G, Collins, MH *et al.* (2008). Efficacy and safety of the oncolytic herpes simplex virus rRp450 alone and combined with cyclophosphamide. *Mol Ther* **16**: 879–885.
27. Bennett, JJ, Delman, KA, Burt, BM, Mariotti, A, Malhotra, S, Zager, J *et al.* (2002). Comparison of safety, delivery, and efficacy of two oncolytic herpes viruses (G207 and NV1020) for peritoneal cancer. *Cancer Gene Ther* **9**: 935–945.
28. Fong, Y, Kim, T, Bhargava, A, Schwartz, L, Brown, K, Brody, L *et al.* (2009). A herpes oncolytic virus can be delivered via the vasculature to produce biologic changes in human colorectal cancer. *Mol Ther* **17**: 389–394.
29. Turner, DL, Cauley, LS, Khanna, KM and Lefrançois, L (2007). Persistent antigen presentation after acute vesicular stomatitis virus infection. *J Virol* **81**: 2039–2046.
30. Sobol, PT, Hummel, JL, Rodrigues, RM and Mossman, KL (2009). PML has a predictive role in tumor cell permissiveness to interferon-sensitive oncolytic viruses. *Gene Ther* **16**: 1077–1087.
31. McFadden, G, Mohamed, MR, Rahman, MM and Bartee, E (2009). Cytokine determinants of viral tropism. *Nat Rev Immunol* **9**: 645–655.
32. Guy, CT, Cardiff, RD and Muller, WJ (1992). Induction of mammary tumors by expression of polyomavirus middle T oncogene: a transgenic mouse model for metastatic disease. *Mol Cell Biol* **12**: 954–961.
33. Koziol, JA, Maxwell, DA, Fukushima, M, Colmerauer, ME and Pilch, YH (1981). A distribution-free test for tumor-growth curve analyses with application to an animal tumor immunotherapy experiment. *Biometrics* **37**: 383–390.
34. Ercolini, AM, Ladle, BH, Manning, EA, Pfannenstiel, LW, Armstrong, TD, Machiels, JP *et al.* (2005). Recruitment of latent pools of high-avidity CD8 (+) T cells to the antitumor immune response. *J Exp Med* **201**: 1591–1602.

35. Wall, EM, Milne, K, Martin, ML, Watson, PH, Theiss, P and Nelson, BH (2007). Spontaneous mammary tumors differ widely in their inherent sensitivity to adoptively transferred T cells. *Cancer Res* **67**: 6442–6450.
36. Mossman, KL and Smiley, JR (1999). Truncation of the C-terminal acidic transcriptional activation domain of herpes simplex virus VP16 renders expression of the immediate-early genes almost entirely dependent on ICP0. *J Virol* **73**: 9726–9733.
37. Chuang, CM, Monie, A, Wu, A, Pai, SI and Hung, CF (2009). Combination of viral oncolysis and tumor-specific immunity to control established tumors. *Clin Cancer Res* **15**: 4581–4588.
38. Qiao, J, Kottke, T, Willmon, C, Galivo, F, Wongthida, P, Diaz, RM *et al.* (2008). Purging metastases in lymphoid organs using a combination of antigen-nonspecific adoptive T cell therapy, oncolytic virotherapy and immunotherapy. *Nat Med* **14**: 37–44.
39. Li, MO, Wan, YY, Sanjabi, S, Robertson, AK and Flavell, RA (2006). Transforming growth factor-βregulation of immune responses. *Annu Rev Immunol* **24**: 99–146.
40. Jarnicki, AG, Lysaght, J, Todryk, S and Mills, KH (2006). Suppression of antitumor immunity by IL-10 and TGF-βproducing T cells infiltrating the growing tumor: influence of tumor environment on the induction of $CD4^+$ and $CD8^+$ regulatory T cells. *J Immunol* **177**: 896–904.
41. Grinshtein, N, Ventresca, M, Margl, R, Bernard, D, Yang, TC, Millar, JB *et al.* (2009). High-dose chemotherapy augments the efficacy of recombinant adenovirus vaccines and improves the therapeutic outcome. *Cancer Gene Ther* **16**: 338–350.
42. Appay, V, Jandus, C, Voelter, V, Reynard, S, Coupland, SE, Rimoldi, D *et al.* (2006). New generation vaccine induces effective melanoma-specific $CD8^+$ T cells in the circulation but not in the tumor site. *J Immunol* **177**: 1670–1678.
43. Obeid, M, Tesniere, A, Ghiringhelli, F, Fimia, GM, Apetoh, L, Perfettini, JL *et al.* (2007). Calreticulin exposure dictates the immunogenicity of cancer cell death. *Nat Med* **13**: 54–61.
44. Ercolini, AM, Machiels, JP, Chen, YC, Slansky, JE, Giedlen, M, Reilly, RT *et al.* (2003). Identification and characterization of the immunodominant rat HER-2/neu MHC class I epitope presented by spontaneous mammary tumors from HER-2/neu-transgenic mice. *J Immunol* **170**: 4273–4280.
45. Bonneau, RH, Salvucci, LA, Johnson, DC and Tevethia, SS (1993). Epitope specificity of H-2Kb-restricted, HSV-1-, and HSV-2-cross-reactive cytotoxic T lymphocyte clones. *Virology* **195**: 62–70.
46. Parkhurst, MR, Fitzgerald, EB, Southwood, S, Sette, A, Rosenberg, SA and Kawakami, Y (1998). Identification of a shared HLA-A*0201-restricted T-cell epitope from the melanoma antigen tyrosinase-related protein 2 (TRP2). *Cancer Res* **58**: 4895–4901.
47. Cai, WZ and Schaffer, PA (1989). Herpes simplex virus type 1 ICP0 plays a critical role in the de novo synthesis of infectious virus following transfection of viral DNA. *J Virol* **63**: 4579–4589.
48. Guy, CT, Webster, MA, Schaller, M, Parsons, TJ, Cardiff, RD and Muller, WJ (1992). Expression of the neu protooncogene in the mammary epithelium of transgenic mice induces metastatic disease. *Proc Natl Acad Sci USA* **89**: 10578–10582.
49. O'Brien, J, Wilson, I, Orton, T and Pognan, F (2000). Investigation of the Alamar Blue (resazurin) fluorescent dye for the assessment of mammalian cell cytotoxicity. *Eur J Biochem* **267**: 5421–5426.
50. Brown, CW, Stephenson, KB, Hanson, S, Kucharczyk, M, Duncan, R, Bell, JC *et al.* (2009). The p14 FAST protein of reptilian reovirus increases vesicular stomatitis virus neuropathogenesis. *J Virol* **83**: 552–561.